Published OnlineFirst May 11, 2016; DOI: 10.1158/1541-7786.MCR-15-0366

Genomics

Molecular Cancer Research

An Integrative Approach Uncovers Biomarkers that Associate with Clinically Relevant Disease Outcomes in Vulvar Carcinoma

Andre M. Lavorato-Rocha[1], Erica M. Akagi[1], Beatriz de Melo Maia[1], Iara S. Rodrigues[1], Mayara Caroline Silva Botelho[1], Fabio A. Marchi[2], Gabriel Fernandes[3], Glauco Baiocchi[4], Fernando A. Soares[5], Silvia Regina Rogatto[2], Yukie Sato-Kuwabara[5], and Rafael M. Rocha[1]

Abstract

Vulvar squamous cell carcinoma (VSCC) is a rare disease that has a high mortality rate (~40%). However, little is known about its molecular signature. Therefore, an integrated genomics approach, based on comparative genome hybridization (aCGH) and genome-wide expression (GWE) array, was performed to identify driver genes in VSCC. To achieve that, DNA and RNA were extracted from frozen VSCC clinical specimens and examined by aCGH and GWE array, respectively. On the basis of the integration of data using the CONEXIC algorithm, PLXDC2 and GNB3 were validated by RT-qPCR. The expression of these genes was then analyzed by IHC in a large set of formalin-fixed paraffin-embedded specimens. These analyses identified 47 putative drivers, 46 of which were characterized by copy number gains that were concomitant with overexpression and one with a copy number loss and downregulation. Two of these genes, *PLXDC2* and *GNB3*, were selected for further validation: PLXDC2 was downregulated and GNB3 was overexpressed compared with non-neoplastic tissue. By IHC, both proteins were ubiquitously expressed throughout vulvar tissue. High expression of GNB3 and low PLXDC2 immunostaining in the same sample was significantly associated with less lymph node metastasis and greater disease-free survival. On the basis of a robust methodology never used before for VSCC evaluation, two novel prognostic markers in vulvar cancer are identified: one with favorable prognosis (GNB3) and the other with unfavorable prognosis (PLXDC2).

Implications: This genomics study reveals markers that associate with prognosis and may provide guidance for better treatment in vulvar cancer. *Mol Cancer Res; 14(8); 720–9. ©2016 AACR.*

Introduction

Vulvar squamous cell carcinoma (VSCC) is an uncommon disease, constituting 3% to 5% of all malignancies in the female genital tract (1, 2). VSCC develops primarily in elderly women, after their 70s; however, the number of cases in younger patients has been climbing, likely due to human papillomavirus (HPV) infection (2).

Despite efforts in the last decade to identify the molecular signature of vulvar cancer, few tumor markers have demonstrated clinical value. Most studies have suggested tumor markers for characterization and VSCC prognostication (3–7). Furthermore, *TP53* mutation and *CDKN2A* promoter methylation have been associated with VSCC (8–11).

Wide-coverage methods, such as chromosomal and array comparative genomic hybridization (aCGH), have been used in several studies to better understand VSCC, reporting gains in 3q and 8q and losses in 3p and 8q as recurrent alterations (12–16). Despite these findings, most of these studies used lower-resolution CGH approaches (12–14); two used FFPE samples, which can lead to data misinterpretation (12, 13); and none validated the observed alterations.

Notably, certain genomic alterations do not affect RNA or protein expression (17). Thus, another technique with wide coverage, such as genome-wide expression (GWE) array, is used to identify driver alterations.

Only one study (18) has used a multimodal approach to compare copy number alterations (CNA) and GWE in VSCC. The study was based on the frequency of CNAs to further compare with GWE. This method has several limitations: the size of the region might contain a large number of genes, and this approach alone fails to determine the actual influence of CNA on changes in gene expression (19). Micci and colleagues selected 2 genes, based on recurrent losses on 3p and 9p by aCGH (*FHIT* and *PTPRD*), and 5 genes (*MAL*, *KRT4*, *OLFM4*, *SPRR2G*, and *S100A7A*), based on expression array alterations. However, none of the gene abnormalities was associated with clinical or pathologic variables.

In this study, we examined a carefully selected subset of VSCC by integrating aCGH and GWE data using validated statistical methods to improve our understanding of vulvar cancer. Our integrative analysis identified 47 candidate drivers for VSCC. Two

[1]Molecular Morphology Laboratory, AC Camargo Cancer Center, São Paulo, Brazil. [2]NeoGene Laboratory, AC Camargo Cancer Center, São Paulo, Brazil. [3]Catholic University of Brasília, Brasilia, Brazil. [4]Department of Gynecology Oncology, AC Camargo Cancer Center, São Paulo, Brazil. [5]Department of Anatomic Pathology, AC Camargo Cancer Center, São Paulo, Brazil.

Note: Supplementary data for this article are available at Molecular Cancer Research Online (http://mcr.aacrjournals.org/).

Corresponding Author: Rafael M. Rocha, AC Camargo Cancer Center, Rua Antônio Prudente, 440, São Paulo, SP 01508-010, Brazil. Phone: 5511-9855-69336; Fax: 5511-2189-5000; E-mail: rafael.malagoli@gmail.com

doi: 10.1158/1541-7786.MCR-15-0366

Published OnlineFirst May 11, 2016; DOI: 10.1158/1541-7786.MCR-15-0366

genes (*PLXDC2* and *GNB3*) were validated and demonstrated a high correlation with the prognosis.

Materials and Methods

Case selection

Seventeen DNA samples of VSCC fresh frozen tissues, with paired RNA (tumoral and adjacent normal tissues), from the Tumor Biobank and 150 formalin-fixed paraffin-embedded (FFPE) samples from the Anatomic Pathology Department, AC Camargo Cancer Center (São Paulo, Brazil), were acquired. DNA and RNA of the frozen tissues were used for aCGH, gene expression, and as well for validation. The amount of quality samples did not allow an independent validation. All samples were obtained from patients who underwent surgery at this institution between 1980 and 2008, and none received neoadjuvant therapy. Furthermore, an experienced pathologist in vulvar diseases carefully reviewed all specimens before the molecular and immunohistochemical analysis.

Clinical data were obtained from the medical records of this institution, and this study was approved by the institutional ethics committee (Protocol # 1623/11). HPV was analyzed using the Linear Array HPV Genotyping Test Kit (Roche Molecular Diagnostics), and the entire technique has been detailed by our group (6).

DNA and RNA extraction

Total RNA was extracted from macrodissected frozen tissue.

Briefly, tissue samples were dissected and lysed, and total RNA was extracted using the RNeasy Mini Kit (QIAGEN) and a Precellys per the manufacturer's instructions to increase the yield of the reaction.

The DNA pellets from the tissue lysis step were incubated with Cell Lysis Solution (Gentra Puregene Blood Kit, QIAGEN) for 18 hours in a thermomixer at 55°C. Then, the reactions were centrifuged, and phenol-chloroform-isoamyl alcohol was added. The reactions were centrifuged sequentially with glycogen at 20 mg/mL and 100% and 70% EtOH. The EtOH was removed, and samples were dried and resuspended in distilled water.

After the quality and quantity of the DNA and RNA were measured, samples with high integrity and quality were used for further analysis.

aCGH

A total of 400 ng of tumor DNA and normal commercially available DNA (Promega) was differentially labeled using the Genomic DNA Enzymatic Labeling Kit (Agilent Technologies). The hybridizations were performed using the SurePrint G3 Human CGH Microarray Kit, 8 × 60K (Agilent Technologies) as per the manufacturer's recommendations. Acquisition of array images and data evaluation were performed as described by Cirilo and colleagues (2013; ref. 20). CNAs were evaluated prior to data integration by NEXUS copy number software version 5.0 (BioDiscovery). For this analysis, the threshold used was 1×10^{-5} with a minimum of 5 consecutive probes altered. Gains were considered when greater than 0.3; high gain (> 0.8); losses (←0.3), and homozygous loss those lower than −1.2.

GWE

Gene expression profiles were evaluated using the SurePrint G3 Human GE 8 × 60K Microarray Platform (Agilent Technologies) as per the manufacturer's protocol. Tumor samples were compared with a pool of 11 adjacent normal tissue samples. The slides were scanned on a DNA microarray scanner with SureScan High-Resolution Technology (Agilent Technologies), and the data were extracted using Feature Extraction v 11.0.1.1 (Agilent Technologies), build 37. TMeV (version 4.8) and R (version 2.15) were used to analyze the gene expression data. Raw data from the array scans were normalized by median-centering of the genes for each array and log2-transformed. Also, probes with low reproducibility were removed using a filter.

Genomic data were deposited into NCBI Gene Expression Omnibus (GEO) and are accessible through GEO Series accession number GSE (http://www.ncbi.nlm.nih.gov/geo/query/acc.cgi?acc=GSE68409).

Integrative analysis

The genomic and transcriptomic data were integrated to identify driver genes and the processes that they influence. These genes were selected using the CONEXIC algorithm, which combines CNAs and gene expression data and constructs regulatory networks, based on the driver genes that appear (19). Also, the algorithm uses a Bayesian function to detect modulator candidates (drivers) among the regions with amplifications and deletions. The ranked score reflects how well a driver candidate predicts the behavior of a module—higher scores increase the likelihood of a gene having an adaptive advantage on the tumor phenotype. The genes that were selected through the integrative analysis were analyzed with regard to functional enrichment using Ingenuity Pathway Analysis (IPA, www.qiagen.com/ingenuity).

Quantitative analysis of DNA copy number (qPCR) and gene expression (RT-qPCR)

DNA copy number was measured using two primer pairs that flanked two regions that were covered by aCGH probes for *PLXDC2* and *GNB3*. The primers were designed using OligoTech, version 1.00 (Oligos Etc. Inc.; Therapeutics Inc). Two endogenous genes were used for normalization: *HPRT* and *GAPDH*. The *PLXDC2* and *GNB3* primer sequences and conditions are described in Supplementary File S1.

The reactions were performed in a MicroAmp Optical 96-Well Reaction Plate (Life Technologies) on an Applied Biosystems 7900HT Fast Real-Time PCR System (Applied Biosystems). Each reaction, performed in triplicate, contained 10 μL Power SYBR Green PCR Master Mix (Life Technologies), 9 μL distilled water, and 0.6 μL each of the forward and reverse primers. Each DNA sequence was quantified and normalized to both endogenous genes. The thresholds for defining a fragment as unaltered (0.5–1.50) and involved in losses (<0.50) and gains (>1.50) were established from the relative copy number values that were obtained in the same control sample for the aCGH.

Gene expression was analyzed by RT-qPCR per the MIQE guidelines (21). cDNA was obtained after reverse transcription of total RNA from tumor and adjacent nontumor samples using the High-Capacity cDNA Reverse-Transcription Kit (Applied Biosystems). Assays that covered the probes included in SurePrint G3 Human GE 8 × 60K Microarray Platform (Agilent Technologies) for *PLXDC2* and *GNB3* were used for gene expression validation among 2 endogenous genes (*GAPDH* and *HPRT*; Hs00929702_m1, Hs01564088_m1, Hs99999905_m1, Hs02800695_m1, respectively). We used the TaqMan (Applied Biosystems) method as per

Published OnlineFirst May 11, 2016; DOI: 10.1158/1541-7786.MCR-15-0366

the manufacturer's protocol on a 7900HT Fast Real-Time PCR System (Applied Biosystems). The relative quantification was calculated using the model that was proposed by Pfaffl (2001; ref. 22).

IHC

One-hundred and fifty FFPE primary invasive VSCC samples were included in a TMA in duplicate for immunohistochemical analysis, as described in Lavorato-Rocha and colleagues (2015; ref. 23). PLXDC2 was probed with 1 μg/mL polyclonal anti-PLXDC2 (Abnova) using the ADVANCE Kit (DAKO). GNB3 was analyzed using 2.5 μg/mL polyclonal anti-GNB3 (LifeSpan Biosciences) using the Universal LSAB+ Kit/HRP, Rabbit/Mouse/Goat (DAKO).

Antigen retrieval was performed in a pressure cooker for 15 minutes in Tris-EDTA pH 9.0. The reactions were visualized with DAB (3,3'-diaminobenzidine) for 5 minutes and counterstained with hematoxylin for 1 minute. All reactions included positive (tonsil and or skin cancer for PLXDC2 and colorectal cancer for GNB3) and negative (omission of primary antibody) controls. Tumoral adjacent normal tissue was submitted to same protocol of staining regarding PLXDC2 and GNB3. The slides were scanned on a Pannoramic 250 Flash II (3DHISTECH Kft), and the stains were quantified using Pannoramic Viewer (3DHISTECH Kft) with the DensitoQuant module, which provides an H-Score from 0 to 300. With regard to survival, scores were categorized as having low (1–99), moderate (100–199), and high expression (200–300). Inverse expression patterns of GNB3 and PLXDC2 were compared (i.e., high GNB3/low PLXDC2 vs. low GNB3/high PLXDC2) and low expression was considered when H-Score < 150 for both proteins.

Statistical analysis

Clinical and pathologic variables and qPCR, RT-qPCR, and IHC results were compared by Mann–Whitney test after Kolmogorov–Smirnov test demonstrate that they required a nonparametric approach. χ^2 test was used to compare high GNB3/low PLXDC2 with low GNB3/high PLXDC2 expression with clinical and pathologic data. The Kaplan–Meier method was used to determine survival rates, and log-rank test was used to calculate RR. Statistics analyses were performed using SPSS version 21.0.0.0 (IBM), considering $P \leq 0.05$ as significant.

Results

Sample characterization

Eighteen VSCC samples were examined by aCGH analysis, 66.7% of which were classified as VSCC grade 1 or 2 and 72.2% of which had FIGO stage I or II. Furthermore, 72.2% of patients had no perineural or vascular invasion, and 55.6% had no nodal metastasis. Most subjects were classified as high-risk HPV-positive (66.7%).

CNAs

Two out of 18 samples used for aCGH analysis did not show significant CNAs. The remaining 16 showed a mean of 234 alterations per sample, ranging from 18 to 573. Events of copy number gains were more frequent than losses; however, all the 16 samples had both events concomitantly. Eleven of them exhibited events of high copy number gains and 4 presented homozygous copy loss (Table 1).

Twenty-eight copy numbers were significantly altered: 22 gains, harboring 506 genes, and 6 losses, encompassing 27 genes. The average length of the alterations was 760 kbp.

The frequency of gains and losses varied from 22% to 55% of samples. Gains in 3q27.1, 3q27.2-q27.3, and 19p13.2 were observed in 44% of samples; 38.9% showed gains in 9q33.3-q34.11, 9q34.11, 11q12.3, 11q13.1, 11q13.1-q13.2, 11q13.2, 11q13.3-q13.4, and 16q22.1; 33.3% had gains in 14q24.3; 27.8% had gains in 7p22.3, 7p22.1, 7q11.23, 7q11.23, 7q22.1, 9p13.3, 9p13.3, 12p13.31, and 18q11.2; and 22% had gains in 15q11.1-11.2. Only the region that mapped to 3p11.1-q11.1 experienced a loss in more than half of all samples (55.6%). The regions that mapped to 9p23 and 10p12.31 had losses in 38.9% of samples, and 18q22.1 was lost in 27.8%. Furthermore, 22.2% of samples had deletions in 18p11.21 and 21p11.2. All the gains and losses are available in Supplementary Files S2.

Gene expression alterations

On the basis of the transcriptomic data, 7,951 genes were significantly altered in tumor samples, excluding replicates. Of these genes, 3,842 were overexpressed and 4,109 were downregulated compared with the pool of adjacent normal tissues. The

Table 1. Type and number of significant genomic CNAs per sample performed in the NEXUS software

	HCNG	CNG	CNL	HCNL	CNG/CNL	HCNG/CNG	HCNL/CNL	Total
V07T 2H	5	497	54	0	1	0	0	557
V09T REP 2LAV	0	0	0	0	0	0	0	0
V15T	0	116	6	0	0	0	0	122
V33T	14	39	85	2	0	0	0	140
V34T	0	481	90	2	0	0	0	573
V12T 2H	63	196	97	0	0	8	0	364
V18T 2H	79	162	31	0	0	0	0	272
V22T 2H	12	184	6	0	0	0	0	202
V13T	3	218	11	0	0	0	0	232
V40T	5	27	5	2	0	0	0	39
V21T	0	16	2	0	0	0	0	18
V30T 2LAV	1	52	25	0	0	0	0	78
V39T	4	455	45	2	0	0	1	507
V20T	0	277	17	0	0	0	0	294
V25T	0	61	16	0	0	0	0	77
V24T	0	0	0	0	0	0	0	0
V27T 2H	14	3	93	0	0	0	0	110
V08T	37	62	55	0	1	0	0	155

Abbreviations: CNG, copy number gain; CNL, copy number loss; CNG/CNL, copy number gain and copy number loss in the same region; HCNG, high copy number gain; HCNL, homozygous copy number loss; HCNG/CNG, high copy number gain and copy number gain in the same region; HCNL/CNL, homozygous copy number loss and copy number loss in the same region.

Published OnlineFirst May 11, 2016; DOI: 10.1158/1541-7786.MCR-15-0366

Table 2. Forty-seven genes selected on the basis of integrated analysis of aCGH and GWE by CONEXIC

CONEXIC rank	Gene symbol	Gene name	CNA	GWE
1	*PAPOLB*	Poly(A) polymerase beta (testis specific)	+	1.16
2	*DPEP2*	Dipeptidase 2	+	1.17
3	*EMG1*	EMG1 N1-specific pseudouridine methyltransferase	+	1.30
4	*PMS2L2*	Postmeiotic segregation increased 2-like 2 pseudogene	+	1.15
5	*CAMK2N2*	Calcium/calmodulin-dependent protein kinase II inhibitor 2	+	2.16
6	*PTMS*	Parathymosin	+	1.28
7	*MICALL2*	MICAL-like 2	+	1.20
8	*TUT1*	Terminal uridylyl transferase 1, U6 snRNA-specific	+	1.52
9	*DUS2L*	Dihydrouridine synthase 2	+	1.58
10	*NSUN5*	NOP2/Sun domain family, member 5	+	1.32
11	*WBSCR22*	Williams Beuren syndrome chromosome region 22	+	1.21
12	*UNC93B1*	Unc-93 homolog B1 (C. elegans)	+	1.20
13	*FAM220A*	Family with sequence similarity 220, member A	+	1.22
14	*EFEMP2*	EGF containing fibulin-like extracellular matrix protein 2	+	1.20
15	*CD72*	CD72 molecule	+	2.73
16	*RHOD*	RAS homolog family member D	+	2.23
17	*CDCA3*	Cell division cycle associated 3	+	2.16
18	*EMID2*	EMI domain containing 2	+	1.39
19	*INTS5*	Integrator complex subunit 5	+	1.32
20	*CCDC85B*	Coiled-coil domain containing 85B	+	1.21
21	*CA9*	Carbonic anhydrase IX	+	4.82
22	*ABCF3*	ATP-binding cassette, sub-family F (GCN20), member 3	+	1.19
23	*LEPREL2*	Leprecan-like 2	+	1.43
24	*ASB6*	Ankyrin repeat and SOCS box containing 6	+	1.20
25	*C11orf68*	Chromosome 11 open reading frame 68	+	1.48
26	***PLXDC2***	**Plexin domain containing 2**	**–**	**-2.20**
27	*STX1A*	Syntaxin 1A (brain)	+	1.32
28	*PACS1*	Phosphofurin acidic cluster sorting protein 1	+	1.21
29	*ANO1*	Anoctamin 1, calcium activated chloride channel	+	1.34
30	*GANAB*	Glucosidase, alpha; neutral AB	+	1.29
31	*CCDC88B*	Coiled-coil domain containing 88B	+	1.17
32	*RPP25L*	Ribonuclease P/MRP 25 kDa subunit-like	+	1.28
33	*HINT2*	Histidine triad nucleotide binding protein 2	+	1.27
34	*GSTP1*	Glutathione S-transferase pi 1	+	1.36
35	*C7orf50*	Chromosome 7 open reading frame 50	+	2.17
36	*SPAG8*	Sperm associated antigen 8	+	1.39
37	*TPI1*	Triosephosphate isomerase 1	+	1.56
38	*TTC9C*	Tetratricopeptide repeat domain 9C	+	1.32
39	*FBXL18*	F-box and leucine-rich repeat protein 18	+	1.23
40	*FANCG*	Fanconi anemia, complementation group G	+	2.13
41	*MACROD1*	MACRO domain containing 1	+	1.16
42	*SSSCA1*	Sjogren syndrome/scleroderma autoantigen 1	+	1.17
43	*ALG3*	ALG3, alpha-1,3-mannosyltransferase	+	1.51
44	*ENO2*	Enolase 2 (gamma, neuronal)	+	2.60
45	*TNRC18*	Trinucleotide repeat containing 18	+	1.23
46	***GNB3***	**Guanine nucleotide binding protein (G protein), beta polypeptide 3**	**+**	**1.23**
47	*CDK2AP2*	Cyclin-dependent kinase 2–associated protein 2	+	1.25

NOTE: The genes are ranked according to score.

average fold change in genes selected normalized by 1 (unaltered reference) varied from −715.57 (*DCD*, dermcidin) to 16.34 (*AMTN*, amelotin), and the raw average fold change in these genes ranged from −8.48 (SD 1.75) to 5.03 (SD 2.45), respectively.

Integrative analysis: Driver candidate selection

Forty-seven driver candidates were selected by the CONEXIC algorithm as the top-ranked genes (Table 2). Only *PLXDC2* (mapping to 10p12.31) had a deletion that was concomitant with downregulation. The other genes had copy number gains and increased expression.

The expression data of the 47 possible drivers was subjected association between them and the clinical and pathologic variables evaluated (Supplementary files S3 and S4).

All 47 genes were subjected to functional enrichment analysis using IPA, revealing the top three networks, associated with carbohydrate metabolism, cellular maintenance, RNA posttranscriptional modification, and organ development (Fig. 1). The pathways and functions that correlated with these genes were examined and confirmed using KOBAS 2.0, as summarized in Supplementary File S5.

The evaluation of gene expression data revealed that only 19 of them were somehow associated with at least one of the clinical and pathologic variables, being *UNC93B1* the gene with the greater number of associations. Therefore, this gene did not appeared in any of our *in silico* analysis, and it was discharged for further validation.

The following strategy was to evaluate those genes with greater number of clinical associations and along with *GNB3* others appeared showing possible relevance in VSCC (Supplementary files S3 and S4). However, of those with higher number of associations with the variables only *GNB3* had association with

Published OnlineFirst May 11, 2016; DOI: 10.1158/1541-7786.MCR-15-0366

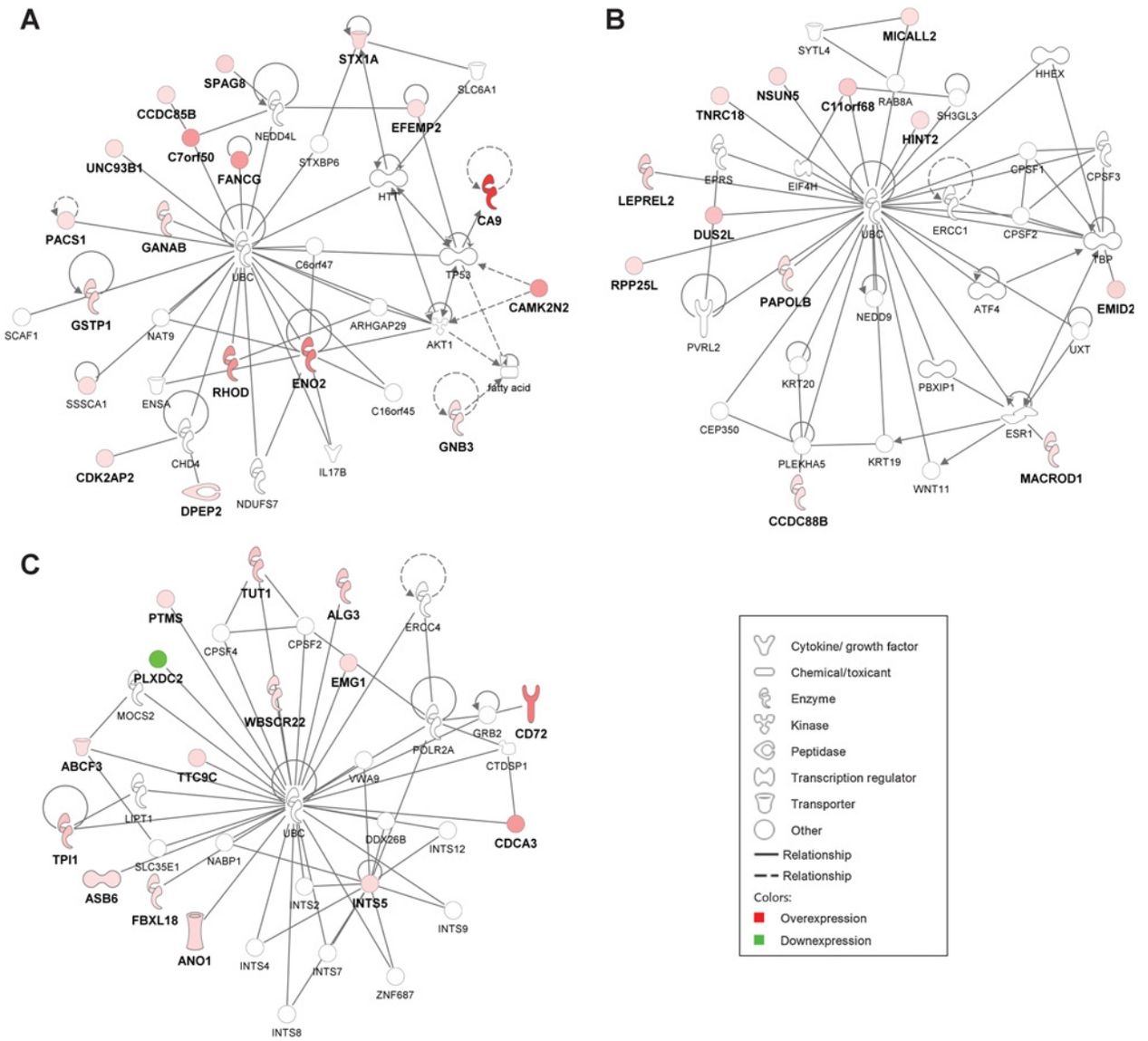

Figure 1.

In silico analysis of top networks based on 47 possible driver genes by IPA. **A–C,** the top networks based on IPA software. The rectangle on the bottom right contains information on molecules regarding their function and expression.

lymph node metastasis, the best prognostic marker so far established. In addition, it was present in the *in silico* evaluation demonstrating its potential in tumoral process. Thus, it was selected for further validation along with *PLXDC2* that presented association with recurrence and more importantly was the only gene that presented loss of copy number associated with gene downregulation.

Data validation by qPCR and RT-qPCR

On the basis of our results, *PLXDC2* had one of the primer pair that corroborated the aCGH findings, with copy number loss (0.197) and the second was normal (0.616). *GNB3* was quantified, with mean copy number ranging from 0.619 to 0.693 (Suplementary File S5). The only significant association between the qPCR results and clinicopathologic features was the correlation of a higher number of copies of the first sequence evaluated of *GNB3* with the presence of lymph node metastasis ($P = 0.03$; Table 3).

Overexpression of *GNB3* (RQ = 2.014; SD = 2.89) and low level of *PLXDC2* (RQ = 0.429; SD = 0.53; Suplementary File S6) versus normal samples were detected by RT-qPCR. However, no association between both genes with clinical and pathologic parameters was observed (Supplementary File S7).

IHC

GNB3 and PLXDC2 were homogeneously expressed throughout the cytoplasm of cells from all vulvar tissue samples (Fig. 2). PLXDC2 and GNB3 evaluation in tumor adjacent normal tissue

Published OnlineFirst May 11, 2016; DOI: 10.1158/1541-7786.MCR-15-0366

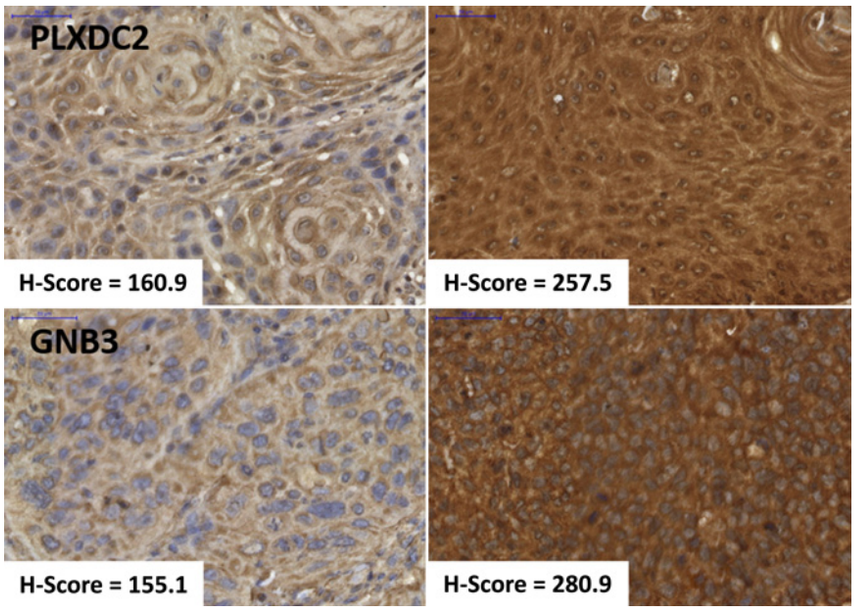

Figure 2.
Immunohistochemical patterns of PLXDC2 and GNB3 proteins based on H-Score evaluation.

demonstrated that both have low expression in nontumoral tissues (Supplementary Files S8).

GNB3 had a median H-Score of 248.42 (range: 155.14–284.08), and that of PLXDC2 was 220.89 (range: 159.75–267.18).

GNB3 immunostaining was significantly higher in VSCC grade 1 and 2 ($P = 0.01$) and trended toward greater expression in cases without vascular invasion ($P = 0.068$; Table 4). PLXDC2 expression was higher in cases without vascular and perineural invasion ($P = 0.011$ and $P = 0.032$, respectively; Table 4).

Patients who expressed more GNB3 experienced higher rates of disease-free survival (DFS). Conversely, high levels of PLXDC2 trended toward lower DFS and cancer-specific survival (CSS; Fig. 3).

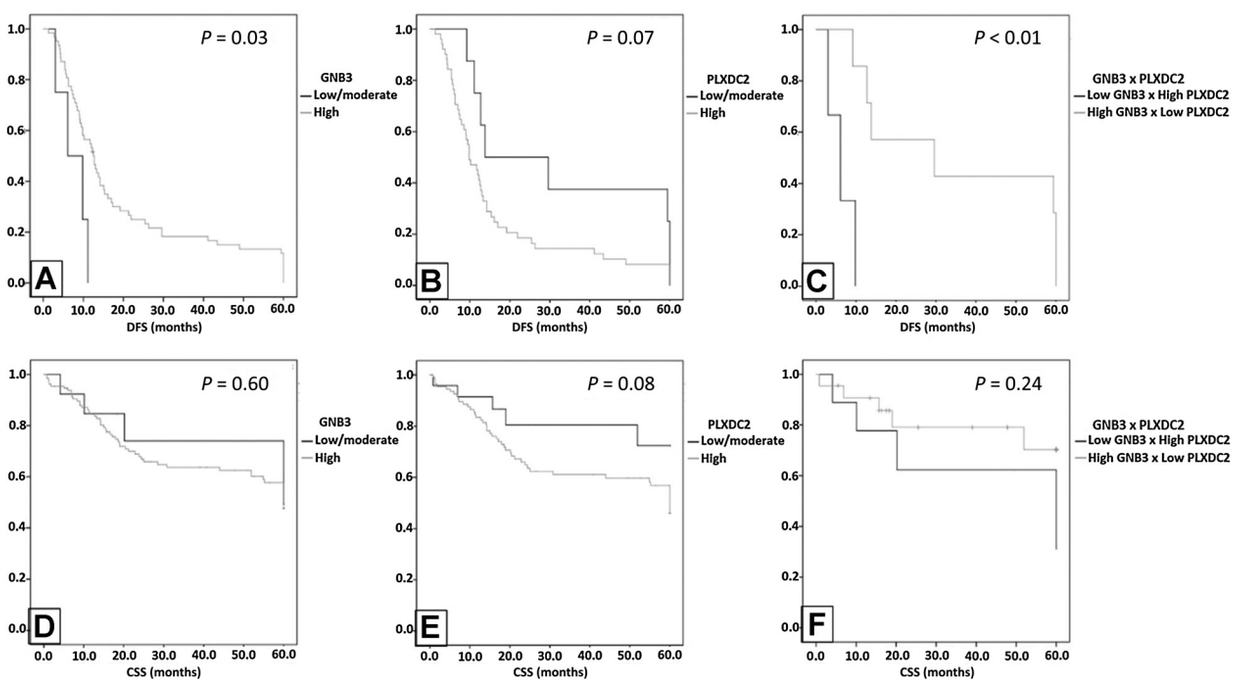

Figure 3.
Cancer-specific (CSS) and disease-free survival (DFS) curves of GNB3 and PLXDC2 protein expression. **A–C,** DFS of GNB3, PLXDC2, and GNB3/PLXDC2, respectively; **D–F,** CSS of GNB3, PLXDC2, and GNB3/PLXDC2, respectively.

Published OnlineFirst May 11, 2016; DOI: 10.1158/1541-7786.MCR-15-0366

Table 3. Significant CNAs and their association with clinical and pathologic variables

	GNB3-1			GNB3-2			PLXDC2-1			PLXDC2-2		
Variables	***N***	**Mean rank**	***P***	***N***	**Mean rank**	***P***	***N***	**Mean rank**	***P***	***N***	**Mean rank**	***P***
Histology												
SCC1/2-Verrucous	6	6.75	0.81	6	7.17	0.52	6	3.92	0.01	6	6.67	0.87
CC3-Basaloid	6	6.25		6	5.83		6	9.08		6	6.33	
Invasion												
Superficial	4	5.88	0.67	4	7.50	0.49	4	6.38	0.93	4	6.00	0.73
Dermis Deep	8	6.81		8	6.00		8	6.56		8	6.75	
Vascular invasion												
Negative	10	7.40	0.23	10	7.75	0.42	10	7.70	0.38	10	6.80	0.07
Positive	6	10.33		6	9.75		6	9.83		6	11.33	
Perineural invasion												
Negative	11	7.23	0.11	11	7.50	0.21	11	8.05	0.57	11	7.23	0.11
Positive	5	11.30		5	10.70		5	9.50		5	11.30	
Lymph node metastasis												
Negative	4	2.75	**0.03**	4	3.50	0.14	4	5.50	0.62	4	4.00	0.33
Positive	5	6.80		5	6.20		5	4.60		5	5.80	
HPV infection												
Negative	5	8.90	0.82	5	6.00	0.16	5	6.10	0.17	5	6.10	0.17
Positive	11	8.32		11	9.64		11	9.59		11	9.59	
FIGO staging												
I–II	9	6.33	0.08	9	6.28	0.07	9	6.44	0.10	9	6.39	0.09
III–IV	6	10.50		6	10.58		6	10.33		6	10.42	
Recrudescence												
Negative	10	7.45	0.94	10	6.85	0.36	10	6.90	0.39	10	6.90	0.40
Positive	4	7.63		4	9.13		4	9.00		4	9.00	

High expression of GNB3, concomitant with low PLXDC2 levels, was detected in cases with little lymph node (0 or 1) metastasis ($P = 0.016$), characterized as FIGO I or II ($P = 0.037$; Table 5), and higher DFS rates ($P = 0.005$; Supplementary Fig. S4).

Discussion

Compared with normal DNA, we observed a few number of copy number losses in vulvar carcinoma samples, which has not been reported. However, most studies are not comparable with our findings, because they extracted DNA from FFPE (12, 13) or cell lines (14, 15). Furthermore, some studies controlled for HPV, used disparate methods or lower-resolution platforms (12–15).

Gains in the long arm of chromosome 3 were frequent in our casuistic, which is a common finding in studies on VSCC (12–15) and other solid tumors (24). However, the normally concomitant findings with this imbalance (e.g., gains in chr8q and losses in chr3p and chr8p) were not observed. These alterations are generally found in solid tumors (24) and might mediate their development and progression (24). Yet, such abnormalities have not been shown to be important in vulvar cancer.

Thus, we proposed a novel approach, performing integrative analyses to identify driver genes that are involved in the initiation

Table 4. Association of H-Score based on protein expression of PLXDC2 and GNB3 and clinical and pathologic variables (Mann–Whitney test)

	PLXDC2		GNB3	
Variables	**Mean rank**	***P***	**Mean rank**	***P***
Histology				
SCC1/2-Verrucous	38.04	0.46	42.39	0.01*
CC3-Basaloid	33.83		27.60	
Invasion				
Superficial	44.37	**0**	42.09	0.09
Dermis deep	26.43		33.56	
Vascular invasion				
Negative	46.40	**0.01**	49.10	0.06
Positive	29.41		36.53	
Perineural invasion				
Negative	44.22	**0.03**	45.79	0.79
Positive	27.45		43.77	
Lymph node metastasis				
Negative	53.67	0.51	57.93	0.61
Positive	57.94		61.32	
HPV infection				
Negative	23.77	0.30	29.10	0.24
Positive	28.10		24.05	
FIGO staging				
I–II	66.27	0.49	72.48	0.99
III–IV	71.04		72.53	

Published OnlineFirst May 11, 2016; DOI: 10.1158/1541-7786.MCR-15-0366

Table 5. Association between inverse expression of PLXDC2 and GNB3 and clinical and pathologic variables (Mann–Whitney)

		Low GNB3 × high PLXDC2	High GNB3 × low PLXDC2	*P*
Histology	SCC1/2-Verrucous	4	12	0.85
	SCC3-Basaloid	2	5	
Vascular invasion	Absent	4	15	0.68
	Present	2	5	
Perineural invasion	Absent	5	16	0.85
	Present	1	4	
Lymph node metastasis	Absent	4	14	0.01
	Present	4	1	
FIGO staging	I+II	4	18	0.03
	III+IV	5	4	
HPV	Negative	1	11	0.27
	Positive	3	6	
Depth of invasion	Superficial and medial dermis	4	4	0.13
	Deep dermis and subcutaneous space	2	13	

and/or progression of VSCC and determine the function of certain regions and genes that have been implicated.

Possible driver selection for VSCC used CONEXIC as starting point for further selection. This method is not a usual method of aCGA and GWE integration as previously used by Micci and colleagues (2013; ref. 16). The CONEXIC methodology uncovers the "genomic footprint" by identifying genes located in regions amplified or deleted in some, but not all tumors and further associates their expression to a gene module, which is assumed to be altered by the driver (19). All this comparisons are made on the basis of validated algorithms which select the best candidate based not only in the assumption that altered copy number is leading to gene misregulation (19). Therefore, although Micci and colleagues (2013) has higher resolution and used similar quantity and quality of samples, this study has major discrepancies in terms of gene selection (16). In addition, this might explain the different pattern of alterations found in both studies as our study follows a different pathway to uncover the main actors in VSCC.

As expected, based on JISTIC analysis, loss of DNA copy number, concomitant with gene downregulation, was uncommon, which we detected in 1 of 47 potential drivers of VSCC. Thus, plexin domain-containing 2 (*PLXDC2*), a 473-kb gene in crh10p12.31, was selected for validation, despite scarce information on its involvement in cancer. Moreover, the lack of reports on its interactions and function might explain its seemingly minor contribution to biologic and molecular disorders, as evaluated *in silico* by IPA.

The enrichment analysis of 47 genes demonstrated that they interact in three principal networks that regulate several functions of cancer development and progression, corroborating their selection as potential drivers. One such molecular influences was the involvement of guanine nucleotide-binding protein (G protein) beta polypeptide 3 (*GNB3*) in carbohydrate metabolism, which is essential for cell growth and maintenance. Thus, *GNB3* was also selected for further validation and evaluation in a larger subset of samples.

PLXDC2, also known as *TEM7R* (tumor endothelial marker 7-related), has a related gene, *PLXDC1*, which was initially termed tumor endothelial marker 7 (*TEM7*; ref. 25). Although *PLXDC2* is usually upregulated with *PLXDC1* in stromal endothelial cells of several tumors, such as colorectal cancer (25), it does not appear to govern endothelial cell morphogenesis in these tumors like *PLXDC1* (25). Instead, *PLXDC2* participates in apoptosis and cell-cycle arrest (26) and is also associated with poor outcomes, a worse prognosis, and lymph node metastasis in breast cancer (27). Regardless of the increasing association of this gene with tumor behavior, its function and interactions have not been examined.

There is significant evidence that supports our assumption that *PLXDC2* and its protein mediate the development and progression of VSCC, primarily in association with GNB3 expression. As observed in this study, low levels of PLXDC2, concomitant with high expression of GNB3, mitigate lymph node metastasis, which is the major prognostic factor of VSCC (28). This association correlates with a better prognosis, because it is related to early-stage tumors (FIGO I and II) and higher DFS rates.

That PLXDC2 does not act as a single modulator is corroborated by the lack of an association of GNB3 alone with lymph node metastasis. *GNB3* is 7 kb and lies at chr12p13. Our study is the first to report the overexpression of GNB3 in cancer, concomitant with copy number gains. The few studies that have analyzed *GNB3* examined the C825T SNP, which is associated with enhanced G protein function, increasing signal transduction through an alternative splice variant, referred to as Gβ3s (29, 30). The behavior of this variant depends on the tumor site. It is a good prognostic factor, reducing the risk of bone metastasis in patients with breast cancer (31) and increasing the survival of patients with glioblastomas (30) but is associated with worse outcomes for patients who carry this SNP, as in head and neck tumors (32).

We could not assume the status of allele 825 of *GNB3*; consequently, further studies might determine whether the upregulation of *GNB3*, concomitant with DNA gains, enhances its G protein activity and whether other alterations are present. Moreover, multimodal approaches (e.g., miRNAs and methylation analysis), integrated with our results, might increase our understanding of VSCC.

Our findings reveal novel aspects of VSCC and tumor behavior. In our previous study, we suggested that p16 is not completely linked with HPV infection, as has been proposed for years, based on the studies of cervix carcinomas, which are almost exclusively related to this infection (5). We hypothesize that there are genes less frequent and studied that mediate VSCC. Thus, our study describes a new model that does not involve the preconceived etiogenic pathways that are linked exclusively to HPV infection or p53 disruption (2, 33), because no gene was associated with either pathway in our analysis. In addition, low expression of both GNB3 and PLXDC2 in normal tissues might reflect their relevance in vulvar carcinogenesis and in tumor progression as they could

Published OnlineFirst May 11, 2016; DOI: 10.1158/1541-7786.MCR-15-0366

reflect a suppression mechanism feedback, imposed by PLXDC2 and a tumoral enhancer promoted by GNB3 expression.

This study proposes two novel genes, based on a robust integrative method that has never been used before to determine the prognosis of vulvar carcinoma. When inversely expressed, *PLXDC2* and *GNB3* predict lymph node metastasis and DFS, guiding the use of a more aggressive treatment modality and increasing the chances of curing VSCC patients.

Disclosure of Potential Conflicts of Interest

No potential conflicts of interest were disclosed.

Authors' Contributions

Conception and design: A.M. Lavorato-Rocha, I.S. Rodrigues, F.A. Soares, R.M. Rocha

Development of methodology: A.M. Lavorato-Rocha, E.M. Akagi, I.S. Rodrigues, M.C.S. Botelho, S.R. Rogatto

Acquisition of data (provided animals, acquired and managed patients, provided facilities, etc.): A.M. Lavorato-Rocha, B. de Melo Maia, I.S. Rodrigues, G. Baiocchi, S.R. Rogatto

Analysis and interpretation of data (e.g., statistical analysis, biostatistics, computational analysis): A.M. Lavorato-Rocha, B. de Melo Maia, F.A. Marchi, G. Fernandes, F.A. Soares, S.R. Rogatto

Writing, review, and/or revision of the manuscript: A.M. Lavorato-Rocha, B. de Melo Maia, I.S. Rodrigues, M.C.S. Botelho, F.A. Marchi, F.A. Soares, S.R. Rogatto, R.M. Rocha

Administrative, technical, or material support (i.e., reporting or organizing data, constructing databases): A.M. Lavorato-Rocha, E.M. Akagi, G. Baiocchi, Y. Sato-Kuwabara

Study supervision: G. Baiocchi, Y. Sato-Kuwabara, R.M. Rocha

Acknowledgments

The authors thank the A.C.Camargo Cancer Center Biobank for providing human specimens.

Grant Support

This study was supported by CNPq, CAPES, and FAPESP.

The costs of publication of this article were defrayed in part by the payment of page charges. This article must therefore be hereby marked *advertisement* in accordance with 18 U.S.C. Section 1734 solely to indicate this fact.

Received August 27, 2015; revised April 5, 2016; accepted April 21, 2016; published OnlineFirst May 11, 2016.

References

1. Stroup AM, Harlan LC, Trimble EL. Demographic, clinical, and treatment trends among women diagnosed with vulvar cancer in U.S. Gynecol Oncol 2008;108:577–83.
2. de Melo Maia B, Munhoz Cestari F, Lavorato-Rocha AM, Sant'Ana Rodrigues I, Baiocchi G, Cardoso Guimarães G, et al. Characterization of socio-demographic and clinicopathological features in Brazilian patients with vulvar squamous cell carcinoma. Gynecol Obstet Invest 2013;75:53–60.
3. Knopp S, Tropè C, Nesland JM, Holm R. A review of molecular pathological markers in vulvar carcinoma: lack of application in clinical practice. J Clin Pathol 2009;62:212–8.
4. Lavorato-Rocha AM, de Melo Maia B, Rodrigues IS, Stiepcich MM, Baiocchi G, da Silva Cestari FM, et al. Prognostication of vulvar cancer based on p14ARF status: molecular assessment of transcript and protein. Ann Surg Oncol 2013;20:31–9.
5. Lavorato-Rocha AM, Rodrigues IS, de Melo Maia B, Stiepcich MM, Baiocchi G, Carvalho KC, et al. Cell cycle suppressor proteins are not related to HPV status or clinical outcome in patients with vulvar carcinoma. Tumour Biol 2013;34:3713–20.
6. Rodrigues IS, Lavorato-Rocha AM, de M Maia B, Stiepcich MM, de Carvalho FM, Baiocchi G, et al. Epithelial-mesenchymal transition-like events in vulvar cancer and its relation with HPV. Br J Cancer 2013;109:184–94.
7. de Melo Maia B, Fontes AM, Lavorato-Rocha AM, Rodrigues IS, de Brot L, Baiocchi G, et al. EGFR expression in vulvar cancer: clinical implications and tumor heterogeneity. Hum Pathol 2014;45:917–25.
8. Gasco M, Sullivan A, Repellin C, Brooks L, Farrell PJ, Tidy JA, et al. Coincident inactivation of 14–3-3sigma and p16INK4a is an early event in vulval squamous neoplasia. Oncogene 2002;21:1876–81.
9. Soufir N, Queille S, Liboutet M, Thibaudeau O, Bachelier F, Delestaing G, et al. Inactivation of the CDKN2A and the p53 tumour suppressor genes in external genital carcinomas and their precursors. Br J Dermatol 2007;156:448–53.
10 Choschzick M, Hantaredja W, Tennstedt P, Gieseking F, Wölber L, Simon R. Role of TP53 mutations in vulvar carcinomas. Int J Gynecol Pathol 2011;30:497–504.
11. Oonk MH, Eijsink JJ, Volders HH, Hollema H, Wisman GB, Schuuring E, et al. Identification of inguinofemoral lymph node metastases by methylation markers in vulvar cancer. Gynecol Oncol 2012;125:352–7.
12. Jee KJ, Kim YT, Kim KR, Kim HS, Yan A, Knuutila S. Loss in 3p and 4p and gain of 3q are concomitant aberrations in squamous cell carcinoma of the vulva. Mod Pathol 2001;14:377–81.
13. Allen DG, Hutchins AM, Hammet F, White DJ, Scurry JP, Tabrizi SN, et al. Genetic aberrations detected by comparative genomic hybridisation in vulvar cancers. Br J Cancer 2002;86:924–8.
14. Raitanen M, Worsham MJ, Lakkala T, Carey TE, Van Dyke DL, Grénman R, et al. Characterization of 10 vulvar carcinoma cell lines by karyotyping, comparative genomic hybridization and flow cytometry. Gynecol Oncol 2004;93:155–63.
15. Huang FY, Kwok YK, Lau ET, Tang MH, Ng TY, Ngan HY. Genetic abnormalities and HPV status in cervical and vulvar squamous cell carcinomas. Cancer Genet Cytogenet 2005;157:42–8.
16. Micci F, Teixeira MR, Scheistrøen M, Abeler VM, Heim S. Cytogenetic characterization of tumors of the vulva and vagina. Genes Chromosomes Cancer 2003;38:137–48.
17. Hyman E, Kauraniemi P, Hautaniemi S, Wolf M, Mousses S. Impact of DNA amplification on gene expression patterns in breast cancer. Cancer Res 2002;62:6240–45.
18. Micci F, Panagopoulos I, Haugom L, Dahlback HS, Pretorius ME, Davidson B, et al. Genomic aberration patterns and expression profiles of squamous cell carcinomas of the vulva. Genes Chromosomes Cancer 2013;52:551–63.
19. Akavia UD, Litvin O, Kim J, Sanchez-Garcia F, Kotliar D, Causton HC, et al. An integrated approach to uncover drivers of cancer. Cell 2010;143:1005–17.
20. Cirilo PDR, Marchi FA, Barros MC, Rocha RM, Domingues MAC, Pontes A, et al. An integrative genomic and transcriptomic analysis reveals potential targets associated with cell proliferation in uterine leiomyomas. PLoS One 2013;8:e57901.
21. Bustin SA, Benes V, Garson JA, Hellemans J, Huggett J, Kubista M, et al. The MIQE guidelines: minimum information for publication of quantitative real-time PCR experiments. Clin Chem 2009;55:611–22.
22. Pfaffl MW. A new mathematical model for relative quantification in real-time RT-PCR. Nucleic Acids Res 2001;29:e45.
23. Lavorato-Rocha AM, Anjos LG, Cunha IW, Vassallo J, Soares FA, Rocha RM. Immunohistochemical assessment of PTEN in vulvar cancer: best practices for tissue staining, evaluation, and clinical association. Methods 2015;77–8:20–4.
24. Albertson DG, Collins C, McCormick F, Gray JW. Chromosome aberrations in solid tumors. Nat Genet 2003;34:369–76.
25. Miller-Delaney SF, Lieberam I, Murphy P, Mitchell KJ. Plxdc2 is a mitogen for neural progenitors. PLoS One 2011;6:e14565.
26. Schwarze SR, Fu VX, Desotelle JA, Kenowski ML, Jarrard DF. The identification of senescence-specific genes during the induction of senescence in prostate cancer cells. Neoplasia 2005;7:816–23.
27. Davies G, Cunnick GH, Mansel RE, Mason MD, Jiang WG. Levels of expression of endothelial markers specific to tumour-associated endothelial cells and their correlation with prognosis in patients with breast cancer. Clin Exp Metastasis 2004;21:31–7.

28. Coulter J, Gleason N. Local and regional recurrence of vulval cancer: management dilemmas. Best Pract Res Clin Obstet Gynaecol 2003;17: 663–81.
29. Siffert W. Effects of the G protein beta 3-subunit gene C825T polymorphism: should hypotheses regarding the molecular mechanisms underlying enhanced G protein activation be revised? Focus on "A splice variant of the G protein beta 3-subunit implicated in disease states does not modulate ion channels". Physiol Genomics 2003;13:81–4.
30. El Hindy N, Adamzik M, Lambertz N, Bachmann HS, Worm K, Egensperger R, et al. Association of the GNB3 825T-allele with better survival in patients with glioblastoma multiforme. J Cancer Res Clin Oncol 2010;136:1423–9.
31. Clar H, Langsenlehner U, Krippl P, Renner W, Leithner A, Gruber G, et al. A polymorphism in the G protein beta3-subunit gene is associated with bone metastasis risk in breast cancer patients. Breast Cancer Res Treat 2008;111:449–52.
32. Lehnerdt GF, Franz P, Bankfalvi A, Grehl S, Jahnke K, Lang S, et al. Association study of the G-protein beta3 subunit C825T polymorphism with disease progression an overall survival in patients with head and neck squamous cell carcinoma. Cancer Epidemiol Biomarkers Prev 2008;17: 3203–7.
33. Hørding U, Junge J, Daugaard S, Lundvall F, Poulsen H, Bock JE. Vulvar squamous cell carcinoma and papillomaviruses: indications for two different etiologies. Gynecol Oncol 1994;52:241–46.

Published OnlineFirst May 11, 2016; DOI: 10.1158/1541-7786.MCR-15-0366

Molecular Cancer Research

An Integrative Approach Uncovers Biomarkers that Associate with Clinically Relevant Disease Outcomes in Vulvar Carcinoma

Andre M. Lavorato-Rocha, Erica M. Akagi, Beatriz de Melo Maia, et al.

Mol Cancer Res 2016;14:720-729. Published OnlineFirst May 11, 2016.